

Delaunay-Rips Paper

Amish Mishra and Francis Motta

August 17, 2021

1 Introduction

Welcome to our paper!

2 Background

2.1 Topological Data Analysis

We are living in an information age where data-driven decision making is a huge area of interest. With so much data at our hands, many questions naturally arise.

- How do we extract relevant information from the data?
- How do we even know what is relevant and what is not?
- If we are unable to visualize large quantities of data, especially data in high dimensions, then how do we know what sort of data set we are inspecting?
- Further, how can we compare information extracted from one data set with another?

These are the sorts of difficult and fascinating questions tackled in the field of Topological Data Analysis (TDA). From the name itself, TDA hints at leveraging ideas borrowed from topology with data analysis techniques to measure and quantify qualitative features of data. At a more nuanced level, TDA appears as the child of Algebraic Topology, Computer Science, Statistics, Data Analysis, and Computational Geometry. Results from each field have found beautiful applications in TDA and have shed new light on applicability of theoretical results from mathematics.

2.2 Simplicial Complexes

The idea behind extracting topological features from a given point-cloud requires there to be a method of assigning some sort of “shape” to the data. Only then are we able to study its associated topological properties. The scenario we face is that we have a finite dimensional metric space out of the point-cloud that we need to assign a shape to. With the human eye, we may be able to make out some appropriate surface our data set can live on. However, this situation pokes at a fundamental question that arises when computing: how can we get a computer to do what a human can do? We need to introduce the idea of a *simplicial complex*, a computational efficient way for a computer to build a surface onto a data set.

Definition 1. A simplicial complex is a collection K of non-empty subsets of a set K_0 such that $\{v\} \in K$ for all $v \in K_0$, and $\tau \subset \sigma$ and $\sigma \in K$ guarantees that $\tau \in K$. The elements of K_0 are called vertices of K , and the elements of K are called simplices. Additionally, we say that a simplex has dimension p or is a p -simplex if it has cardinality of $p + 1$. We use K_p to denote the collection of p -simplices. The k -skeleton of K is the union of the sets K_p for all $p \in \{0, 1, \dots, k\}$. If τ and σ are simplices such that $\tau \subset \sigma$, then we call τ a face of σ , and we say that τ is a face of σ of codimension k' if the dimensions of τ and σ differ by k' . The dimension of K is defined as the maximum of the dimensions of its simplices. A map of simplicial complexes, $f : K \rightarrow L$, is a map $f : K_0 \rightarrow L_0$ such that $f(\sigma) \in L$ for all $\sigma \in K$. [EH10]

2.3 Simplicial Homology

2.4 Vietoris-Rips Complex

One of the simplest ways to build a complex on a data set X is by considering the pairwise distance between the points. The approach described here is an algorithmic, bottom-up approach that adds higher and higher dimensional simplices to the complex for a fixed scale. For a given scale $\varepsilon > 0$, if $d(x, x') \leq 2\varepsilon$ for $x, x' \in X$, then we add the edge between x and x' into our complex. Once all of the edges are added, we add the higher dimensional simplices if their faces are already in the complex. That is, we add the k -simplex $\sigma = \{x_0, x_1, \dots, x_k\}$ to the complex if every subset $u \subset \sigma$ is already in the complex. Formally, we define the Vietoris-Rips complex [Ott+17] for scale $\varepsilon > 0$

$$VR_\varepsilon(X) = \{\sigma \subseteq X \mid d(x, x') \leq 2\varepsilon, \forall x, x' \in \sigma\}.$$

2.5 Delaunay Triangulation

Although the Vietoris-Rips complex is simple to implement, constructing it on data sets with large numbers of points results in computation drawback. As the scale increases, we see that adding certain simplices does not affect the homology of the point cloud. We need some way to “weed” out these extraneous simplices as we construct our complex to increase computational efficiency. Turning to a tool of Computational Geometry, we incorporate the Delaunay Triangulation in our construction. Our definition is adapted from “A roadmap for the computation of persistent homology” [Ott+17]. Assume our data X lives in the space \mathbb{R}^n . Let $x \in X$. We define

$$V_x = \{p \in \mathbb{R}^d \mid d(p, x) \leq d(p, x') \ \forall x' \in X\}.$$

Each V_x is called a Voronoi cell. Note that $\{V_x\}_{x \in X}$ forms a cover of \mathbb{R}^n . This cover is known as the Voronoi decomposition of \mathbb{R}^n with respect to X . To construct the Delaunay triangulation from this cover, we connect $x, x' \in X$ with an edge if V_x and $V_{x'}$ are neighbors (that is, the Voronoi cells share a wall). When the points in X are in general position, this gives us a graph (1-skeleton) on X that is known as the Delaunay Triangulation. Formally, we define [EH10]

$$Del(X) = \{\sigma \subset X \mid \bigcap_{u \in \sigma} V_u \neq \emptyset\}.$$

In this paper, we will be only be using the edges of the Delaunay Triangulation. We call it the Delaunay 1-skeleton and define it as

$$Del_1(X) = \{\sigma \in Del(X) \mid \dim(\sigma) = 1\}.$$

We will use $Del_1(X)$ as the underlying graph structure when defining the Delaunay-Rips complex in section 3.1.

2.6 Persistence

3 Delaunay-Rips Complex

3.1 Definition and Construction

The Delaunay-Rips complex is our new method of building a complex on a data set X . The idea is similar to the construction of the Delaunay-Čech complex defined in [BE16]. Delaunay-Rips utilizes the conceptual simplicity of the Vietoris-Rips complex while cutting down on the number of high dimensional and extraneous simplices. This computational speed-up is by virtue of using the Delaunay Triangulation as the “backbone” of building the Vietoris-Rips complex on X . The idea is that we build the Vietoris-Rips complex on X but only add edges if the edges occur in the Delaunay 1-skeleton of the point cloud. The higher dimensional k -simplices are then added the traditional way they are in section 2.4. Formally, we define the Delaunay-Rips Complex for a given scale $\varepsilon > 0$

$$DR_\varepsilon(X) = \{\sigma \subseteq X \mid d(x, x') \leq 2\varepsilon, \ \forall x, x' \in \sigma \text{ and } \sigma \in Del_1(X)\}.$$

3.2 Example Data Set

1. Demonstrate construction on a small data-set (5-8 point data-set).

3.3 Run-time Analysis Comparison

1. How does this scale as dimensions are increased?
2. How does this scale as points are added?

3.4 Persistence Diagram Instability

The Delaunay-Rips construction gains computational efficiency at the cost of stability. We demonstrate a simple, yet clear example of how this instability can arise. In figure 1, we can visually see a particular configuration of four points giving a radically different Persistence Diagram as we move the right-most point across the circumcircle of the other 3 points. In the figure, we have marked the Delaunay Triangulation of the points to show case the point at which an edge flip occurs (namely when all four points lie on the same circle). We now proceed to formally prove the instability of this particular configuration of points.

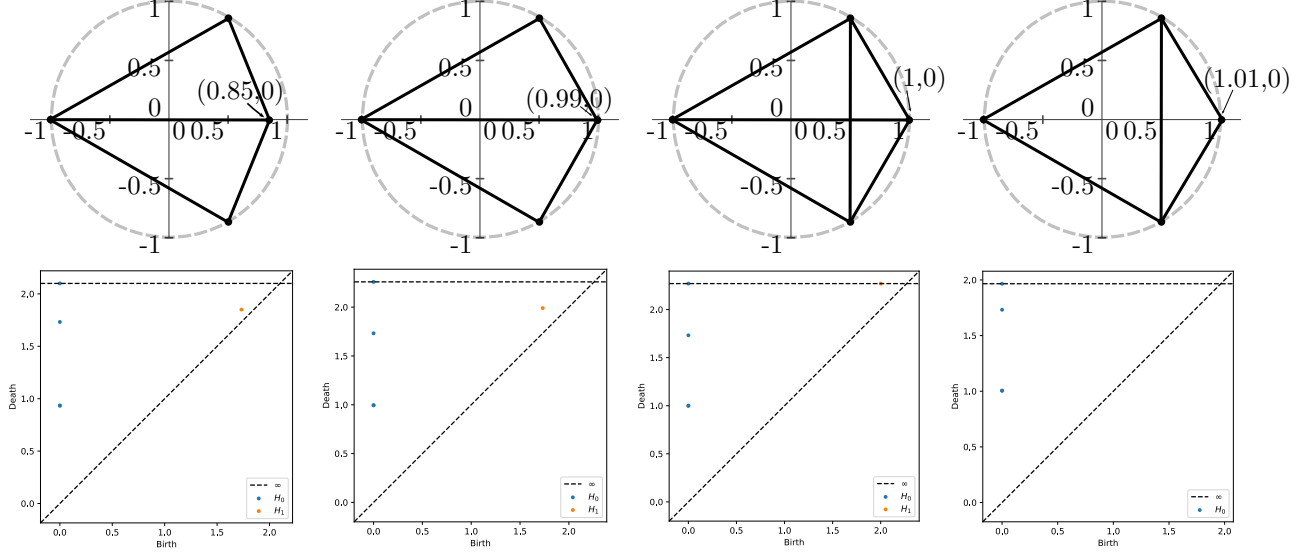


Figure 1: Persistence Diagrams of 4 point example

Let (\mathcal{P}, d_{GH}) be the space of point clouds equipped with the Gromov-Hausdorff metric and let (\mathcal{D}, W_∞) be the space of Persistence Diagrams equipped with the bottle neck metric. Define

$$\varphi : \mathcal{P} \rightarrow \mathcal{D}$$

$$\varphi(P) := Pers(P)$$

where $Pers(P)$ is the persistence diagram of the point cloud P constructed using the Delaunay-Rips complex. Our example comes from 4 points taken in \mathbb{R}^2 where the instability is demonstrated as the discontinuity of φ .

Let $P \in \mathcal{P}$ as $P = \{(-1, 0), (\frac{1}{2}, \frac{\sqrt{3}}{2}), (\frac{1}{2}, -\frac{\sqrt{3}}{2}), (1, 0)\}$. Note that the points all lie on the unit circle, so the Delaunay 1-skeleton has an edge between every pair of points (See figure). Thus, $\varphi(P)$ has no H_1 class with non-zero persistence using the Delaunay-Rips filtration, as can be verified by the reader.

Fix $\varepsilon = 0.1$. We now show that for any $\delta > 0$, there exists $P' \in \mathcal{P}$ such that $d_{GH}(P, P') < \delta$, but $W_\infty(\varphi(P), \varphi(P')) \geq \varepsilon$. Take $P' = \{(-1, 0), (\frac{1}{2}, \frac{\sqrt{3}}{2}), (\frac{1}{2}, -\frac{\sqrt{3}}{2}), (1 - x, 0)\}$ with $0 < x < \delta < \frac{2 - \sqrt{3}}{2}$. This is a small perturbation of P by pushing the point $(1, 0)$ inside the unit circle thereby putting the points in general position. We only work with $\delta < 2 - \sqrt{3}$ so that $\varphi(P')$ maintains an H_1 class with non-zero persistence; for this example to work, we further need $\delta < \frac{2 - \sqrt{3}}{2}$. We just compute the Hausdorff distance d_H between P and P' in the plane taking the isometric embedding of P to be the map that sends each of its points to itself in \mathbb{R}^2 and the same embedding for P' . Since the Gromov-Hausdorff distance is the infimum of $d_H(f(P), g(P'))$ over all isometric embeddings $f : P \rightarrow X$ and $g : P' \rightarrow X$ into any metric space X , $d_H(P, P')$ serves as an upper bound for $d_{GH}(P, P')$. We find that

$$d_{GH}(P, P') \leq d_H(P, P') = x < \delta.$$

Recall that $\varphi(P)$ has no H_1 class with non-zero persistence. Thus, to compute $W_\infty(\varphi(P), \varphi(P'))$, we must match the H_1 class of $\varphi(P')$ with the diagonal. The H_1 class of $\varphi(P')$ has birth $\sqrt{3}$ and death $2 - x$ as calculated in the Appendix, section 6.1. Using the max norm, we find

$$d := W_\infty(\varphi(P), \varphi(P')) = 2 - x - \sqrt{3} \geq 2 - \frac{2 - \sqrt{3}}{2} - \sqrt{3} \geq 0.1 = \varepsilon.$$

Hence, our map φ is discontinuous at P . This gives us insight into when the Delaunay-Rips construction of the Persistence Diagram experiences instability—namely when points are not in general position. We now have motivation to ask if we have stability of the PD when the underlying Delaunay-Rips complex does not change under a perturbation of the point cloud.

3.5 Stability in a Neighborhood

1. What is the best our method can do? Use knowledge on stability of Delaunay Triangulation. Let P denote our point cloud and P' denote the perturbed point cloud. We use $|xy|$ notation to denote the Euclidean distance between points $x, y \in \mathbb{R}^n$. Let V_x denote the closed Voronoi region for the point $x \in P$. Here is a lemma that should work in \mathbb{R}^n :

Lemma 3.1. *Two points $p_i, p_j \in P$ are strong Voronoi neighbors if and only if there exists an m such that*

$$\max\{|mp_i|, |mp_j|\} < \min_{k \neq i, j} |mp_k|.$$

We claim

Theorem 3.2. *Let $p_i, p_j \in P$ be strong Voronoi neighbors and $m \in V_{p_i} \cap V_{p_j}$. For $\varepsilon = \min\{\frac{1}{4}(\min_{k \neq i, j} |mp_k| - |mp_j|), \frac{1}{2} \min_{i \neq j} |p_i p_j|\}$, an ε -perturbation of P leaves p_i and p_j as strong Voronoi neighbors.*

Proof. Let $p_i, p_j \in P$ satisfy Lemma 3.1 with $m \in V_{p_i} \cap V_{p_j}$. Note that $0 < \varepsilon < \frac{1}{2} \min_{i \neq j} |p_i p_j|$ to ensure a unique correspondence between the points of P and the points of P' . We begin with the conclusion of Lemma 3.1:

$$\begin{aligned} \max\{|mp_i|, |mp_j|\} &< \min_{k \neq i, j} |mp_k| \\ 2 \max\{|mp_i|, |mp_j|\} &< 2 \min_{k \neq i, j} |mp_k| \\ \min_{k \neq i, j} |mp_k| + 3 \max\{|mp_i|, |mp_j|\} &< 3 \min_{k \neq i, j} |mp_k| + \max\{|mp_i|, |mp_j|\} \\ \frac{1}{4} \min_{k \neq i, j} |mp_k| + \frac{3}{4} \max\{|mp_i|, |mp_j|\} &< \frac{3}{4} \min_{k \neq i, j} |mp_k| + \frac{1}{4} \max\{|mp_i|, |mp_j|\} \\ \max\{|mp_i|, |mp_j|\} + \frac{1}{4} (\min_{k \neq i, j} |mp_k| - \max\{|mp_i|, |mp_j|\}) &< \min_{k \neq i, j} |mp_k| - \frac{1}{4} (\min_{k \neq i, j} |mp_k| - \max\{|mp_i|, |mp_j|\}) \\ \max\{|mp_i|, |mp_j|\} + \varepsilon &\leq \max\{|mp_i|, |mp_j|\} + \frac{1}{4} (\min_{k \neq i, j} |mp_k| - \max\{|mp_i|, |mp_j|\}) \\ &< \min_{k \neq i, j} |mp_k| - \frac{1}{4} (\min_{k \neq i, j} |mp_k| - \max\{|mp_i|, |mp_j|\}) \leq \min_{k \neq i, j} |mp_k| - \varepsilon. \end{aligned} \tag{1}$$

Now, without loss of generality, let

$$|mp'_i| = \max\{|mp'_i|, |mp'_j|\}.$$

We note by the triangle inequality that

$$\max\{|mp'_i|, |mp'_j|\} \leq |mp_i| + |p_i p'_i| \leq \max\{|mp_i|, |mp_j|\} + \varepsilon. \tag{2}$$

Similarly, we have by the triangle inequality

$$\min_{k \neq i, j} |mp_k| - \varepsilon = \min_{k \neq i, j} (|mp_k| - \varepsilon) \leq \min_{k \neq i, j} (|mp_k| - |p_k p'_k|) \leq \min_{k \neq i, j} |mp'_k|. \tag{3}$$

Putting together equations 1, 2, 3, we have

$$\max\{|mp'_i|, |mp'_j|\} \leq \max\{|mp_i|, |mp_j|\} + \varepsilon < \min_{k \neq i,j} |mp_k| - \varepsilon \leq \min_{k \neq i,j} |mp'_k|.$$

Thus, we now apply Lemma 3.1 and have that p'_i and p'_j remain strong Voronoi neighbors. \square

Alternate attempt at proof:

To keep things simple, we work with our point cloud $P \subset \mathbb{R}^2$ with the idea being

- (a) Assume that the points of P are in general position and affinely independent
 - i. No 4 points lie on the same circle
 - ii. No 3 points lie on the same line
- (b) Look at 3 points, $p_1, p_2, p_3 \in P$ and find the circumcircle, $C_{p_1 p_2 p_3}$ through them.
 - i. This circle must have a finite radius and finite circumcenter by assumption of affine independence
- (c) Embark on a mission to find ε around each point in P such that an ε -perturbation of P , call it P' , ensures all other points $p'_k \in P'$ stayed inside $C_{p'_1 p'_2 p'_3}$ if $p_k \in P$ was inside $C_{p_1 p_2 p_3}$ to begin with or stayed outside if $p_k \in P$ was outside of $C_{p_1 p_2 p_3}$ to begin with.
 - i. We must ensure that there is an ε so that the points in P' are affinely independent—this ensures that moving the points of P within the ε balls around each point of P only cause continuous changes in membership of p_k relative to $C_{p_1 p_2 p_3}$.
 - A. Let $O_1 \in \mathbb{R}^2$ denote the circumcenter of the circle $C_{p_1 p_2 p_3}$. Since the points of P are affinely independent, O_1 is not infinite in any of its coordinates. We can specifically calculate O_1 by finding the intersection of the perpendicular bisectors of $\overline{p_1 p_2}$ and $\overline{p_1 p_3}$. We proceed by linear algebra. The process is
 - Find midpoint of line segment (\mathbf{r}_0)
 - Find directional vector based at the midpoint that points at one of the ends of the line segments (this acts as the normal vector \mathbf{n} to the perpendicular bisector)
 - Find the equation of the perpendicular bisector using

$$\mathbf{n} \cdot \mathbf{r} = \mathbf{n} \cdot \mathbf{r}_0.$$

Once the equations of all necessary perpendicular bisectors are found, we can easily check if they have a solution by checking the determinant of the 2×2 matrix

$$\begin{pmatrix} \mathbf{n}_{p_1 p_2} & \mathbf{n}_{p_1 p_3} \end{pmatrix}$$

Since the normal vectors are just the directional vectors based at the midpoint pointing towards one of the ends of the line segments, we have that

$$\mathbf{n}_{p_i p_j} = p_j - \frac{p_j - p_i}{2} = \frac{p_j + p_i}{2}.$$

Coming back to our example of $C_{p_1 p_2 p_3}$ and letting $p_i = (p_{i1}, p_{i2})$, we now construct the following sequence of maps:

$$\mathbb{R}^2 \times \mathbb{R}^2 \times \mathbb{R}^2 \xrightarrow{f} \mathcal{M}_{2 \times 2}(\mathbb{R}) \cong \mathbb{R}^4 \xrightarrow{\det} \mathbb{R}$$

where

$$f(p_1, p_2, p_3) := ((p_{21} - p_{11})/2, (p_{22} - p_{12})/2, (p_{31} - p_{11})/2, (p_{32} - p_{12})/2)$$

and \det is the standard determinant function. Let $A = ((p_{21} - p_{11})/2, (p_{22} - p_{12})/2, (p_{31} - p_{11})/2, (p_{32} - p_{12})/2)$. Since the determinant is a continuous map, we have that for $\varepsilon = \det(A)/2$, there exists a δ_1 around A such that $\det(A) < \varepsilon$ when $\|A\| < \delta_1$ for each $f_i \in \mathbb{R}^4$. Since f is continuous in each of its components, f itself is continuous. Thus, there exists δ_2 around each p_1, p_2, p_3 such that $f(p_1, p_2, p_3) < \delta_1$ whenever $|p_i| < \delta_2$.

We have found a neighborhood δ_2 around each point p_1, p_2, p_3 that ensures the points do not become collinear.

- ii. We must ensure that there is an ε so that the points in P' are in general position—this ensures that no p_k change membership relative to $C_{p_1 p_2 p_3}$.

4 Application of Delaunay-Rips

1. Demonstrate value by talking about as dimensions change and number of points change.
2. Particular examples of how using special data sets affect the run-time of Rips/Alpha drastically but maybe not Del-Rips.
3. Performance: accuracy in ML algorithm, or classification. Instability may cause performance to go down even though run-time is unaffected.

4.1 Synthetic Data

4.2 Real Data

5 Conclusion

5.1 Further Questions

6 Appendix

6.1 Boundary Matrix Calculation for Instability

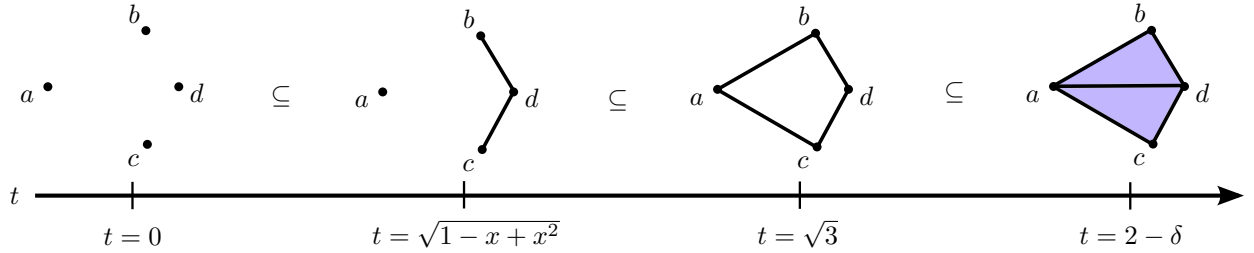


Figure 2: filtration

We have $P' = \{(-1, 0), (\frac{1}{2}, \frac{\sqrt{3}}{2}), (\frac{1}{2}, -\frac{\sqrt{3}}{2}), (1-x, 0)\}$ with $0 < x < \delta < 2 - \sqrt{3}$. Our filtration has 4 key scale values, $t = 0 < \sqrt{1-x+x^2} < \sqrt{3} < 2-\delta$ as shown in Figure 2. We construct our boundary matrix B and reduce it to \bar{B} using the standard algorithm:

$$B = \begin{matrix} & \begin{matrix} a & b & c & d & bd & cd & ab & ac & ad & abd & acd \end{matrix} \\ \begin{matrix} a \\ b \\ c \\ d \\ bd \\ cd \\ ab \\ ac \\ ad \\ abd \\ acd \end{matrix} & \begin{pmatrix} 0 & 0 & 0 & 0 & 0 & 0 & 1 & 1 & 1 & 0 & 0 \\ 0 & 0 & 0 & 0 & 1 & 0 & 1 & 0 & 0 & 0 & 0 \\ 0 & 0 & 0 & 0 & 0 & 1 & 0 & 1 & 0 & 0 & 0 \\ 0 & 0 & 0 & 0 & 1 & 1 & 0 & 0 & 1 & 0 & 0 \\ 0 & 0 & 0 & 0 & 0 & 0 & 0 & 0 & 0 & 1 & 0 \\ 0 & 0 & 0 & 0 & 0 & 0 & 0 & 0 & 0 & 0 & 1 \\ 0 & 0 & 0 & 0 & 0 & 0 & 0 & 0 & 0 & 1 & 0 \\ 0 & 0 & 0 & 0 & 0 & 0 & 0 & 0 & 0 & 0 & 1 \\ 0 & 0 & 0 & 0 & 0 & 0 & 0 & 0 & 0 & 1 & 1 \\ 0 & 0 & 0 & 0 & 0 & 0 & 0 & 0 & 0 & 0 & 0 \\ 0 & 0 & 0 & 0 & 0 & 0 & 0 & 0 & 0 & 0 & 0 \end{pmatrix} \end{matrix}$$

$$\overline{B} = \begin{matrix} & a & b & c & d & bd & cd & ab & ac & ad & abd & acd \\ \begin{matrix} a \\ b \\ c \\ d \\ bd \\ cd \\ ab \\ ac \\ ad \\ abd \\ acd \end{matrix} & \begin{pmatrix} 0 & 0 & 0 & 0 & 0 & 0 & 1 & 0 & 0 & 0 & 0 & 0 \\ 0 & 0 & 0 & 0 & 1 & 1 & 1 & 0 & 0 & 0 & 0 & 0 \\ 0 & 0 & 0 & 0 & 0 & 1 & 0 & 0 & 0 & 0 & 0 & 0 \\ 0 & 0 & 0 & 0 & 1 & 0 & 0 & 0 & 0 & 0 & 0 & 0 \\ 0 & 0 & 0 & 0 & 0 & 0 & 0 & 0 & 0 & 0 & 1 & 1 \\ 0 & 0 & 0 & 0 & 0 & 0 & 0 & 0 & 0 & 0 & 0 & 1 \\ 0 & 0 & 0 & 0 & 0 & 0 & 0 & 0 & 0 & 0 & 1 & 1 \\ 0 & 0 & 0 & 0 & 0 & 0 & 0 & 0 & 0 & 0 & 0 & 1 \\ 0 & 0 & 0 & 0 & 0 & 0 & 0 & 0 & 0 & 0 & 1 & 0 \\ 0 & 0 & 0 & 0 & 0 & 0 & 0 & 0 & 0 & 0 & 0 & 0 \\ 0 & 0 & 0 & 0 & 0 & 0 & 0 & 0 & 0 & 0 & 0 & 0 \end{pmatrix} \end{matrix}.$$

The persistence pairs for the H_0 class with their persistence diagram coordinate (birth/death pair) come out as follows:

$$\begin{aligned} (a, N/A) &: (0, \infty) \\ (b, ab) &: (0, \sqrt{3}) \\ (c, cd) &: (0, \sqrt{1-x+x^2}) \\ (d, bd) &: (0, \sqrt{1-x+x^2}). \end{aligned}$$

The H_1 classes come out as

$$\begin{aligned} (ad, abd) &: (2-x, 2-x) \\ (ac, acd) &: (\sqrt{3}, 2-x). \end{aligned}$$

The only point with non-zero persistence is $(\sqrt{3}, 2-x)$.

6.2 Pseudo-code Implementation

6.3 Github Repo of Actual, Clean Code

1. We want to compare the best implementation of Del-Rips with Ripser and Cechmate's Alpha.

6.4 Machine Specs

1. Eluktronics laptop

7 Bibliography

Whole bibliography

- [EH10] Herbert Edelsbrunner and John Harer. *Computational Topology: An Introduction*. Jan. 2010. ISBN: 978-0-8218-4925-5. DOI: 10.1007/978-3-540-33259-6_7.
- [BE16] Ulrich Bauer and Herbert Edelsbrunner. “The Morse theory of Čech and Delaunay complexes”. In: *Transactions of the American Mathematical Society* 369.5 (Dec. 2016), pp. 3741–3762. ISSN: 1088-6850. DOI: 10.1090/tran/6991. URL: <http://dx.doi.org/10.1090/tran/6991>.
- [Ott+17] Nina Otter et al. “A roadmap for the computation of persistent homology”. In: *EPJ Data Science* 6.17 (2017). DOI: <https://doi.org/10.1140/epjds/s13688-017-0109-5>.